54.36; H, 6.80; S, 19.19. ^{1}H NMR (C_6D_6): δ 5.83 (s, 10 H, Cp), 4.14 (q, 2 H, J(H-H) = 6.9 Hz, CH_2), 3.01 (septet, 1 H, J(H-H) = 6.8 Hz, CH), 1.43 (d, 6 H, Me), 1.02 (t, 3 H, CH_2CH_3).

$Cp_2Ti(OEt)(SSCMe_3)$ (5c). Yield: 1.24 g, 58%, as an oil. Anal. Calcd for $C_{16}H_{24}OS_2Ti$: C, 55.80; H, 7.02; S, 18.62. Found: C, 55.63; H, 7.11; S, 18.72. ^{1}H NMR (C_6D_6): δ 5.88 (s, 10 H, Cp), 4.16 (q, 2 H, J(H-H) = 6.8 Hz, CH_2), 1.50 (s, 9 H, Me), 1.06 (t, 3 H, CH_2CH_3).

$Cp_2Ti(OEt)(SSCH_2Ph)$ (5d). Yield: 0.44 g, 28%. Mp: 84-86 °C. Anal. Calcd for $C_{19}H_{22}OS_2Ti$: C, 60.31; H, 5.86; S, 16.94. Found: C, 60.15; H, 5.80; S, 17.10. ^{1}H NMR (C_6D_6): δ 7.38-6.69 (m, 5 H, C_6H_5), 5.77 (s, 10 H, Cp), 4.13 (q, 2 H, J(H-H) = 6.9 Hz, CH_2CH_3), 3.95 (s, 2 H, CH_2Ph), 1.00 (t, 3 H, CH_3).

Bis(η-cyclopentadienyl)(chloro)((triphenylmethyl)disulfanido)titanium(IV), $Cp_2Ti(Cl)(SSCPh_3)$ (6). The compound Ph_3CSSCl (1.64 g, 4.79 mmol) was added to a solution of **1** (1.12 g, 4.79 mmol) in toluene (30 mL) at -78 °C. The temperature of the stirred reaction mixture was allowed to rise slowly to 22 °C over a period of 2.5 h. A deep purple powder was obtained after filtration and washing (hexanes, 2 × 10 mL). Addition of the washings to the mother liquors, with cooling to -16 °C, gave a second crop of powder. Flash chromatography on deactivated alumina (1 × 6 cm), eluting with CH_2Cl_2, gave a purple band. The eluate was stripped to dryness and then recrystallized from CH_2Cl_2 layered with hexanes to give a deep purple powder (yield 1.48 g, 54%; mp 155-157 °C dec). Anal. Calcd for $C_{29}H_{25}S_2ClTi \cdot {}^1/_2CH_2Cl_2$: C, 62.88; H, 4.65; S, 11.38. Found: C, 63.14; H, 4.65; S, 11.71. ^{1}H NMR (C_6D_6): δ 7.72-6.98 (m, 15 H, C_6H_5), 5.72 (s, 10 H, Cp).

Acknowledgment. Support for this research from the Natural Sciences and Engineering Council of Canada and the Quebec Department of Education is gratefully acknowledged. S.M. thanks the Canadian Commonwealth Scholarship and Fellowship Plan for a predoctoral scholarship.

Contribution from the Inorganic Chemistry Laboratory, University of Oxford, South Parks Road, Oxford OX1 3QR, U.K.

^{13}C and ^{31}P CP/MAS NMR Studies of the Polytopal Ligand Rearrangement Process of Tungsten Tris(trimethylphosphine) Hexahydride in the Solid State

Stephen J. Heyes, Malcolm L. H. Green, and Christopher M. Dobson*

Received October 24, 1990

$W(PMe_3)_3H_6$ (**1**), an archetypal nine-coordinate transition-metal complex, has been studied in the crystalline state by variable-temperature ^{13}C and ^{31}P CP/MAS NMR spectroscopy. The NMR spectra are consistent with a tricapped-trigonal-prismatic geometry for the complex, with two phosphine ligands in eclipsed prismatic sites and the third capping the prismatic face opposite the other two. The two prismatic phosphines are shown to be on inequivalent sites. At temperatures above 340 K, exchange broadening shows the occurrence of ligand functionality interchange between the different phosphine environments. Analysis of these line shapes and magnetization-transfer data, in the slow limit of exchange, for both ^{13}C and ^{31}P nuclei shows activation parameters of E_a = 148.8 ± 15 kJ mol^{-1} and $A = 6.6 \times 10^{23}$ s^{-1} for the ligand-functionality-interchange process. The most likely mechanism involves a "double-rearrangement" mechanism with polyhedral edge stretches through a monocapped-square-antiprismatic geometry to a tricapped-trigonal-prismatic intermediate in which all phosphines occupy capping positions. This allows complete scrambling of the ligand functionality, in a manner such that the spatial movement of the phosphine ligands within the crystalline frame need only be relatively small. An additional dynamic process, involving a "tripod" reorientation of the PMe_3 rotors, has been detected by dipolar broadening of the ^{13}C NMR spectra. This process is rapid at room temperature but slows to a rate of ca. 10^5 Hz at the lowest temperature studied, 169 K. The reorientation appears to be slightly more facile in the prismatic environments than in the capping position.

Introduction

For complexes with nine identical ligands, the idealized tricapped-trigonal-prismatic (TTP) geometry (point group D_{3h}) is found from experimental studies to be conclusively favored over the alternative monocapped-square-antiprismatic (MSA) arrangement (point group C_{4v}).[1] In accord with this, calculations based on the interligand repulsion potentials, $E = \sum r_{ij}^{-n}$ (n = 1, 2, ..., 6, i ≠ j), show the TTP polytope to be of lower energy for all forms of the potential, and the MSA geometry lies above with no evidence of a minimum.[1] Transition-metal complexes with nine-coordinate geometries about the metal atom are, however, always fluxional in solution; a facile path for interchange of ligands in the TTP structure has been suggested to be via the MSA arrangement, and $D_{3h} \rightleftharpoons C_{4v} \rightleftharpoons D_{3h}$ rearrangement is generally invoked to explain the ligand-scrambling processes. The energy barrier to such interchange would be low, since only slight distortion of the TTP ligand polyhedron, namely stretching of a single polyhedral edge, is required to attain the MSA geometry,[1] as shown in Figure 1. Indeed, the polytopal rearrangements that equilibrate the ligand environments have in general been observed to be in the fast-exchange limit, even at the lowest temperatures attainable in solution NMR studies, suggesting very low barriers to ligand site interchange; line shape data have not been obtained from solution NMR studies, from which to attempt to ascertain possible permutational mechanisms for the ligand scrambling. Available structural data, which favor rigid TTP geometries,[1] suggest that in solids the barriers to polytopal rearrangement are considerably higher than those pertaining in solution, or those calculated by considering merely the *intra*molecular repulsion potential. Solid-state NMR spectroscopy might, therefore, allow exploration of these reorientational processes at lower rates and thus provide mechanistic information.

A particularly interesting case of nine-coordinate geometry is provided by the group of compounds $W(P)_3H_6$, where (P) represents a phosphine ligand. Low-temperature single-crystal X-ray and neutron diffraction studies of the complex $W(PPh(^iPr)_2)_3H_6$[2,3] show a geometry clearly distinct from the idealized TTP (D_{3h}) structure with the three phosphorus atoms occupying the capping sites originally predicted for such compounds.[4,5] The structure is, however, much closer to TTP than to MSA, with two phosphorus atoms in eclipsed prismatic sites and the third residing in the capping position of the prismatic face opposite the other two phosphorus atoms[2,3] (see Figure 2). The phosphorus atoms in the prismatic environments show bond lengths to tungsten that are approximately 0.1 Å longer than the W-P bond length for

(1) Guggenberger, L. J.; Muetterties, E. L. *J. Am. Chem. Soc.* **1976**, *98*, 7221-7225.
(2) Gregson, D.; Howard, J. A. K.; Nicholls, J. N.; Spencer, J. L.; Turner, D. G. *J. Chem. Soc., Chem. Commun.* **1980**, 572-573.
(3) Gregson, D.; Mason, S. A.; Howard, J. A. K.; Spencer, J. L.; Turner, D. G. *Inorg. Chem.* **1984**, *23*, 4103-4107.
(4) Meakin, P.; Guggenberger, L. J.; Peat, W. G.; Muetterties, E. L.; Jesson, J. P. *J. Am. Chem. Soc.* **1973**, *95*, 1467-1474.
(5) Bau, R.; Carroll, W. E.; Hart, D. W.; Teller, R. G.; Koetzle, T. F. *Adv. Chem. Ser.* **1977**, *167*, 73-92.

0020-1669/91/1330-1930$02.50/0

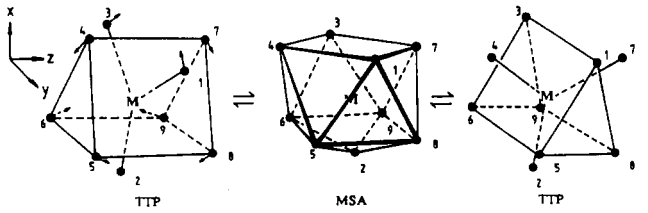

Figure 1. Interchange of TTP and MSA coordination geometries for a nine-coordinate transition-metal complex by means of polyhedral distortion.

the capping phosphorus atom, and the tungsten and phosphorus atoms lie almost in a plane with bond angles P_{pr}–W–P_{ca} > P_{pr}–W–P_{pr}, leading to an overall coordination symmetry of the tungsten atom of C_{2v} in its immediate coordination sphere (the maximum overall molecular symmetry is only C_s). The ^{31}P solution NMR spectrum shows a single narrow resonance at room temperature, but when the temperature is lowered to 180 K, two resonances with the intensity ratio of 1:2 are observed.[2] This low-temperature NMR spectrum is consistent with the structure determined in the crystalline state by the diffraction studies. To account for the fluxionality in solution indicated by the ^{31}P and ^1H NMR spectra at higher temperatures, two dynamic processes were proposed.[2] First, a low-energy "breathing" motion averages the chemical shifts of the different phosphorus and proton nuclei but does not alter the topological relationship of individual hydrogen and phosphorus atoms. Second, a higher energy polytopal rearrangement permutes the hydrogen atoms with respect to the phosphine ligands.

In order to explore further such rearrangements, the closely related compound $W(PMe_3)_3H_6$ (**1**) has been studied in this work in the crystalline state by a combination of ^{31}P and ^{13}C CP/MAS NMR spectroscopy. Trimethylphosphine ligands were chosen in the hope that their relatively small bulk might allow fluxional behavior in the crystalline state, with rates appropriate for analysis of the mechanism of rearrangement. A room-temperature crystal structure for this compound[6] suggests that the disposition of the phosphine ligands about the tungsten atoms is very similar to the case for the (P) = $PPh(^iPr)_2$ analogue, although the hydride atoms were not located. This structure contains a mirror plane through the W–P_{ca} bond such that the prismatic phosphine ligands are symmetry related.

Experimental Section

Preparation of $W(PMe_3)_3H_6$. All compounds were handled on a dual vacuum/nitrogen line by using standard Schlenk techniques[7] and in a drybox containing an inert nitrogen atmosphere. All solvents were predried over molecular sieves, and in addition toluene was then distilled from potassium and petroleum ether (bp 40–60 °C) from a sodium/potassium alloy. Solution ^1H NMR spectra were recorded at 300 MHz on a Bruker WH300 or AM300 spectrometer. Air-sensitive samples were made up under an inert dry nitrogen atmosphere and sealed under vacuum. All spectra were referenced internally to TMS (δ = 0) by using the solvent resonance.

$WCl_4(PMe_3)_3$ was prepared by interaction of WCl_6 with PMe_3 in toluene. **1** was synthesized by treatment of $WCl_4(PMe_3)_3$ with $LiAlH_4$ in diethyl ether, followed by addition of methanol at −78 °C and recrystallization from petroleum ether (bp 40–60 °C) at −80 °C.[8] It was characterized by ^1H NMR spectroscopy in benzene-d_6.

Solid-State NMR Spectroscopy. All solid-state NMR spectra were recorded on a Bruker CXP200 pulse NMR spectrometer with an Oxford Instruments 4.7-T wide-bore (98 mm) superconducting solenoid magnet (200.13 MHz for ^1H NMR) and equipped with an Aspect 2000 data system. ^{13}C and ^{31}P CP/MAS NMR spectra were recorded at 50.32 and 80.96 MHz, respectively, with the use of a multinuclear, proton-enhanced, double-bearing magic angle sample spinning probe (Bruker Z32-DR-MAS-7DB) and a high-power proton decoupler. A single contact spin-lock CP sequence[9] with alternate cycle spin-temperature inversion

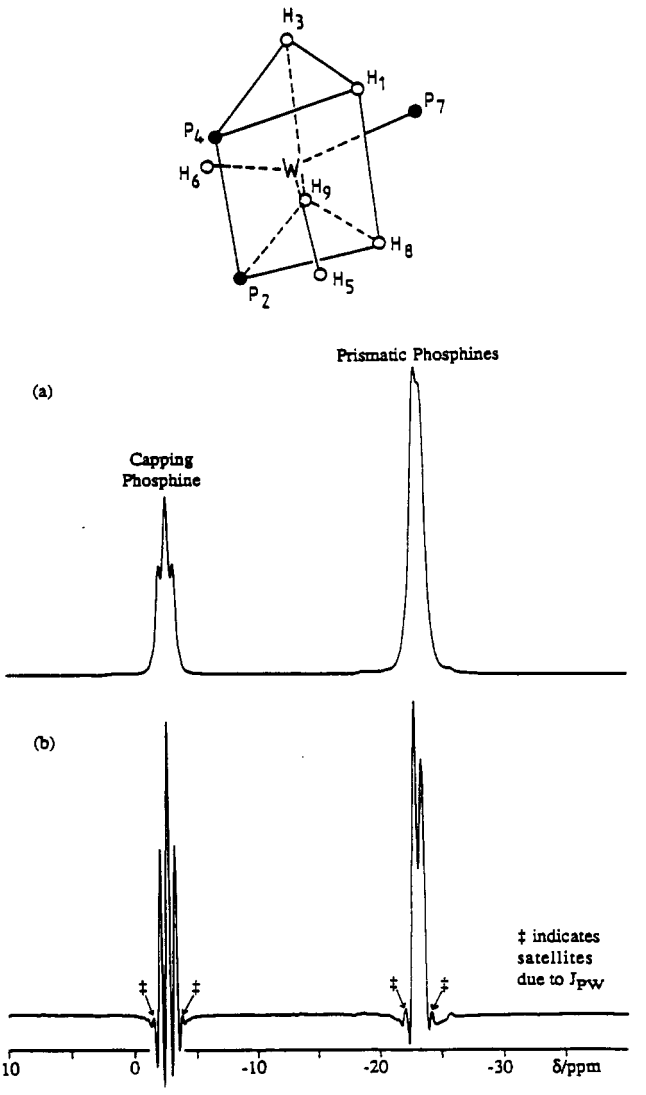

Figure 2. ^{31}P CP/MAS NMR spectrum of $W(PMe_3)_3H_6$ at 296 K showing (a) the isotropic region and (b) the same region processed with resolution enhancement. Inset: proposed TTP geometry for the compounds $W(P)_3H_6$ with two phosphine ligands in eclipsed prismatic sites and the third in the opposite capping site, as determined for (P) = $PPh(^iPr)_2$ by neutron diffraction studies.[3]

and flip back of ^1H magnetization[10] and a proton radio frequency field of 1.7 mT (ω_1 = 72 kHz), resulting in a 90° pulse length of 3.5 μs, was used. Temperature regulation, utilizing a Bruker B-VT1000 unit equipped with a copper–constantan thermocouple and digital reference, was of the bearing gas and temperature measurement was of the bearing exhaust close to the sample. Temperature calibration below room temperature was achieved with the samarium ethanoate Curie law chemical shift thermometer[11] previously calibrated against the phase transition of *d*-camphor[11] and above room temperature with the phase transitions of cobaltocenium hexafluorophosphate[12] and 1,4-diazabicyclo[2.2.2]octane.[11] The system was allowed to equilibrate at each new temperature for 1 h before spectral accumulation was commenced. The setting of the spinner angle was checked at each temperature by using the ^{79}Br resonance of a small amount of KBr,[13] separated from the sample by a plastic disk. Approximately 350 mg of **1** was packed into a 7-mm zirconia rotor with a Kel-F top under an inert atmosphere of dry nitrogen. ^{13}C and ^{31}P CP/MAS NMR spectra were recorded at a range of temperatures from 169 to 381 K. Typically MAS rotation rates were ≈3 kHz, though some ^{31}P NMR spectra were recorded at MAS rotation rates of ≈1.4 and ≈4.5 kHz. Typically, 100–300 transients, with a contact time of 3 ms for ^{13}C

(6) Berry, A. D.Phil. Thesis, University of Oxford, 1987; pp 58–60, 328–329.
(7) Shriver, D. F. *The Manipulation of Air-Sensitive Compounds*; McGraw-Hill: New York, 1969.
(8) Parkin, G. D.Phil. Thesis, University of Oxford, 1987; pp 327–328.
(9) Pines, A.; Gibby, M. G.; Waugh, J. S. *J. Chem. Phys.* **1973**, *59*, 569–590.
(10) Tegenfeld, J.; Haeberlen, U. *J. Magn. Reson.* **1986**, *69*, 191–195.
(11) Haw, J. F.; Campbell, G. C.; Crosby, R. C. *Anal. Chem.* **1986**, *58*, 3172–3177 and references therein.
(12) Heyes, S. J.; Clayden, N. J.; Dobson, C. M.; Wiseman, P. J. Unpublished results.
(13) Frye, J. S.; Maciel, G. E. *J. Magn. Reson.* **1982**, *48*, 125–131.

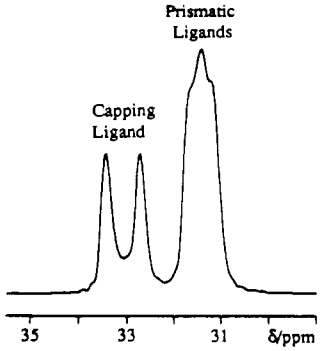

Figure 3. ^{13}C CP/MAS NMR spectrum of $W(PMe_3)_3H_6$ at 296 K.

NMR studies and 1.5 ms for ^{31}P NMR studies and a relaxation delay of 5 s for both, were accumulated for each spectrum. Chemical shifts are reported on the δ scale with respect to $\delta(TMS) = 0$ via the secondary reference, adamantane, for ^{13}C NMR and $\delta(H_3PO_4) = 0$ for ^{31}P NMR. The principal components of chemical shift tensors were recovered from the spinning sideband manifold, measured in at least two slow spinning speed MAS NMR spectra, by using both the Maricq and Waugh moment analysis[14] and the Herzfeld and Berger graphical analysis.[15] The MAS NMR spectrum at each MAS rate was simulated by using eq 30 of Maricq and Waugh[14] to evaluate the MAS FID from the tensor information.[16] Powder averaging was performed in 2° steps, and the rotational echo was replicated to give 1024 points; the FID was convoluted with Gaussian and Lorentzian functions of choice and zero-filled to 8K or 16K points. Iterative comparison of the experimental and simulated MAS NMR spectra was then used for refinement of the tensor components,[16,17] and such refined values are quoted with error limits derived from the fitting process. The Herzfeld–Berger[15] convention for the labeling of sidebands is employed here. The conventional assignment for labeling of the principal components of the CSA tensor is used,[18] employing $\delta_{11} \geq \delta_{22} \geq \delta_{33}$ in order to indicate use of the δ chemical shift scale. The parameter $\Delta = (\delta_{11} - \delta_{33})$ is used as a measure of the spread of the CSA powder pattern and, together with the asymmetry parameter, $\eta = (\delta_{11} - \delta_{22})/(\delta_i - \delta_{33})$ if $(\delta_i - \delta_{33}) > (\delta_{11} - \delta_i)$ but $\eta = (\delta_{22} - \delta_{33})/(\delta_{11} - \delta_i)$ if $(\delta_i - \delta_{33}) < (\delta_{11} - \delta_i)$ (where $0 < \eta < 1$), characterizes any changes to the CSA caused by motional averaging. Magnetization-transfer experiments used the rotationally synchronized, selective magnetization-transfer experiment of Conner et al.,[19,20] which monitors longitudinal polarization transfer between two selected resonances. In each ^{13}C NMR experiment the MAS rotation rate was adjusted such that the evolution time of the experiment was an integral number of spinner rotation periods.[21] Rotational synchronization in the case of ^{31}P NMR studies required unattainably high MAS rotation rates; the maximum possible MAS rate (≈5.5 kHz) was therefore used to cause the greatest possible averaging of the CSA. Kinetic data were obtained from the magnetization data following the analysis of Jeener et al.[22] for spin exchange between two sites of unequal population. For the ^{13}C NMR experiments performed here, magnetization transfer due to spin diffusion could be neglected,[23] and the rate of chemical exchange was obtained directly from the rate of magnetization transfer. For the ^{31}P NMR experiments the temperature-independent contribution due to spin diffusion was determined and subtracted from the rate of magnetization transfer to yield the rate of the chemical-exchange process. The program DNMR4 (QCPE No. 466)[24] was used to calculate the exchange-broadened line shapes for coupled spin systems from the static (chemical shifts, coupling constants, and equilibrium populations of each of the accessible configurations of the system) and dynamic (relaxation and exchange matrices) input parameters in a full-density-matrix treatment.

Table I. ^{31}P NMR Chemical Shift Data for $W(PMe_3)_3H_6$ at 296 K

	δ_i/ppm	δ_{11}/ppm	δ_{22}/ppm	δ_{33}/ppm
capping phosphorus	−2.65	37.6 ± 7.0	12.2 ± 9.0	−57.7 ± 6.0
prismatic phosphorus	−23.15	−1.0 ± 2.0	−1.0 ± 3.0	−67.4 ± 3.0

Results

(a) Analysis of the ^{13}C and ^{31}P CP/MAS NMR Spectra. The ^{13}C and ^{31}P CP/MAS NMR spectra of **1** at room temperature are shown in Figures 2 and 3. The ^{31}P NMR spectrum, which is well resolved ($\Delta\nu_{1/2} < 50$ Hz), may be interpreted on the basis of the known crystal structures, as being indicative of two phosphorus environments with chemical shifts of −2.65 and −23.15 ppm in the intensity ratio of 1:2. These resonances can be assigned to a single capping phosphorus and two eclipsed, essentially equivalent, prismatic phosphorus atoms in the expected TTP structure. The two resonances appear mutually scalar coupled with a coupling constant of $J_{PP} = 48$ Hz (typical for a two-bond J_{PP} coupling), such that the resonance at −2.65 ppm of relative intensity 1 is a triplet (coupled to two equivalent phosphorus atoms) and the resonance at −23.15 ppm is a doublet (coupled to a single phosphorus atom). The components of the doublet appear, however, not to have identical line widths and their peak heights are slightly different. In addition, both resonances have very weak shoulders of similar extension to both low and high frequency. Resolution enhancement reveals these to be low-intensity peaks, which are interpreted as satellites due to J coupling of the ^{31}P to the 14% natural abundance of ^{183}W. Analysis reveals values of $J_{PW} = 92$ and 117 Hz for the resonances at −23.15 and −2.65 ppm, respectively. These spectral parameters compare with the ^{31}P solution NMR spectrum, where a single resonance of chemical shift −18.55 ppm with tungsten satellites of $J_{PW} = 73$ Hz is observed.[25] The chemical shift value in solution compares reasonably well with the weighted mean of solid-state NMR shifts (−16.35 ppm), but the value of the J coupling differs significantly from those observed in the solid state; such couplings are, however, known to be very sensitive to bonding and molecular geometry parameters.[26] The resonance at −2.65 ppm has a greater CSA than does the resonance at −23.15 ppm (see Table I), illustrating the different bonding environments for the phosphine ligands corresponding to the two resonances.

The ^{13}C CP/MAS NMR spectrum shows the excellent resolution typical of methyl group resonances ($\Delta\nu_{1/2} < 12$ Hz). Like the ^{31}P NMR spectrum, the ^{13}C NMR spectrum shows two regions with intensities in the ratio of 1:2. In addition to the possible inequivalence of the phosphine sites, each methyl group on each phosphorus atom is potentially inequivalent; all methyl carbon resonances are therefore potentially nondegenerate. In fact, the spectrum is considerably simplified from this situation in that "tripod" reorientation of the phosphine ligand (i.e. dynamic disorder of the ligand between its three equivalent orientations in the molecule) is sufficiently rapid on the NMR time scale at even the lowest temperature studied here, such that the three methyl groups of a single phosphine are rendered equivalent. At temperatures below 245 K, the ^{13}C CP/MAS NMR resonances appear somewhat broadened (see Figure 4). This broadening may reasonably be interpreted as due to the reorientation process slowing to a rate comparable to the frequency of the proton radio frequency decoupling field ($\omega_1 \approx 72$ kHz) used in these experiments.[27] The maximum line broadening due to this mechanism is expected when $\omega_1\tau_c \approx 1$. The carbon resonance centered at 31.4 ppm apparently broadens substantially only at lower temperatures than does the resonance centered at 33.1 ppm. Methyl groups

(14) Maricq, M. M.; Waugh, J. S. *J. Chem. Phys.* **1979**, *70*, 3300–3316.
(15) Herzfeld, J.; Berger, A. E. *J. Chem. Phys.* **1980**, *73*, 6021–6030.
(16) Clayden, N. J.; Dobson, C. M.; Lian, L.-Y.; Smith, D. J. *J. Magn. Reson.* **1986**, *69*, 476–487.
(17) As discussed in ref 16, the distinction between axial and near-axial tensors is only possible in special cases.
(18) Mehring, M. *Principles of High Resolution NMR in Solids*, 2nd ed.; Springer-Verlag: Berlin, 1983; pp 25–30.
(19) Conner, C.; Naito, A.; Takegoshi, K.; McDowell, C. A. *Chem. Phys. Lett.* **1985**, *113*, 123–128.
(20) Takegoshi, K.; McDowell, C. A. *J. Am. Chem. Soc.* **1986**, *108*, 6852–6857.
(21) Szeverenyi, N. M.; Bax, A.; Maciel, G. E. *J. Am. Chem. Soc.* **1983**, *105*, 2579–2582.
(22) Jeener, J.; Meier, B. H.; Bachmann, P.; Ernst, R. R. *J. Chem. Phys.* **1979**, *71*, 4546–4553.
(23) VanderHart, D. L. *J. Magn. Reson.* **1987**, *72*, 13–47.
(24) Bushweiler, C. H.; Letendre, L. J.; Brunelle, J. A.; Bilofsky, H. S.; Whalon, M. R.; Fleischman, S. H. Quantum Chemistry Program Exchange Program, Program No. 466, "DNMR4".
(25) Lyons, D.; Wilkinson, G. *J. Chem. Soc., Dalton Trans.* **1985**, 587–590.
(26) If the nature of the conformations present is dependent upon temperature, the J-values which reflect these differences would be expected to be also temperature-dependent.
(27) Rothwell, W. P.; Waugh, J. S. *J. Chem. Phys.* **1981**, *74*, 2721–2732.

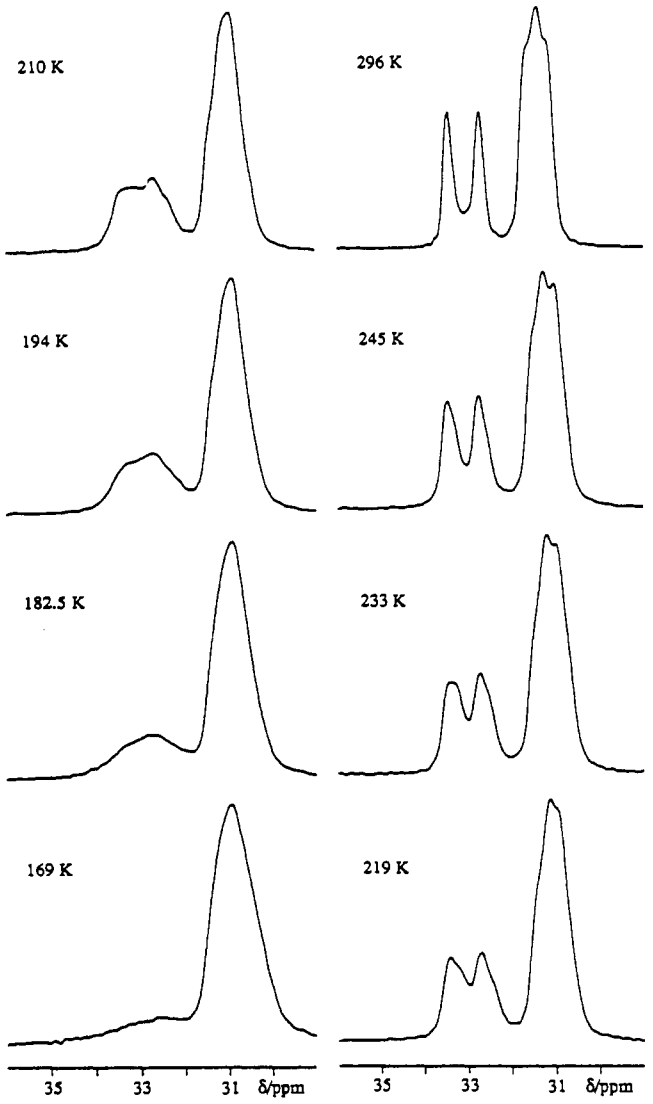

Figure 4. ^{13}C CP/MAS NMR spectra of $W(PMe_3)_3H_6$ in the temperature range 169–296 K.

are generally "tightly coupled" dipolar systems such that each methyl carbon spin is most strongly dipolar-coupled to those protons to which it is directly bonded and only loosely coupled to other proton spins. This has the result that each resonance in the ^{13}C NMR spectrum is only affected by dynamics directly involving the methyl groups which it represents. Thus we may conclude that the reorientation of the trimethylphosphine ligand is slightly more facile in the prismatic environments than in the capping position. Temperatures sufficiently low to measure the region of maximum broadening were not attained, and so calculation of kinetic data for these reorientations did not prove possible.

The fine structure resolved in the ^{13}C NMR resonances of the room-temperature spectrum can be identified as arising from J coupling to phosphorus nuclei. The resonance centered at 33.1 ppm presents itself as a straightforward doublet, suggesting J coupling of the methyl carbons of the capping phosphine only to the directly bonded phosphorus atom, although the intensity of the NMR line shape is noted to be slightly greater between the doublet peaks than expected from spectral simulations. Presumably, the three-bond, vicinal J coupling constants for coupling to the prismatic phosphorus atoms are too small for additional fine structure to be observed. The resonance centered at 31.4 ppm apparently consists of three closely spaced peaks. The central peak is appreciably broader than the outer peaks and is of slightly greater intensity. Furthermore, the frequency separations between each outer peak and the central peak are not exactly equal, accounting for the very slightly asymmetric appearance of the spectrum. Indeed, at different temperatures, the form of this methyl resonance changes very subtly (see Figure 5). At decreasing temperatures below 296 K, the separation of the peak of lowest chemical shift of the trio from the central peak increases relative to the analogous separation for the peak of highest chemical shift and the asymmetry of the resonance becomes more pronounced. Above 296 K, the order of resonance separations is reversed such that the separation of the peak of lowest chemical shift from the central peak becomes the larger, and increasingly so at higher temperatures. The chemical shifts of the methyl resonances of the spectrum are temperature-dependent, moving to higher chemical shifts with increase in temperature. The asymmetry observed in the ambient-temperature spectrum is thus seen to be significant. Such an observation cannot be easily rationalized on the basis of the coupling of a single methyl environment to two phosphorus atoms. However, if the two prismatic phosphine ligands are not in fact structurally equivalent, such that the ^{31}P CP/MAS NMR spectrum merely reflects an accidental near-degeneracy in the chemical shifts of inequivalent phosphine ligands, the form of the ^{13}C NMR resonance centered at 31.4 ppm may be interpreted as being actually a superposition of the two resonances due to the methyl groups of the distinct prismatic phosphines, each showing direct J coupling to phosphorus very similar in magnitude to the other. If the resonances of the two types of methyl groups undergo very slightly different temperature-dependent chemical shifts, this will lead to the experimentally observed changes in the overlap pattern from the doublet resonances due to each methyl type. It is evident, however, that any proposed differences in the prismatic phosphine environments must be very small, and the NMR data are still consistent with a structure with eclipsed prismatic phosphines, as found in the diffraction studies; this illustrates the manner in which NMR isotropic chemical shifts are an extremely sensitive probe of local structure. The existence of slightly inequivalent prismatic phosphine ligands also explains the apparent anomalies noticed in the ^{31}P NMR spectra; the different line widths in the resonance of the doublet centered at −23.15 ppm become understandable on this basis. As is the case in the ^{13}C NMR studies, the ^{31}P NMR chemical shifts are somewhat temperature-dependent, leading to the subtle changes observed in the fine structure of the resonances (vide infra), which are well explained on the above model. It is well-known in many other systems that methyl groups, because of their frequent location in the vicinity of intermolecular contacts, act as amplifiers of crystallographic effects. Thus, despite the larger ^{31}P NMR chemical shift range, we might expect any slight nonequivalence of phosphine ligands to be most apparent in the ^{13}C NMR signals of the methyl carbons.[28]

(b) Analysis of Ligand-Functionality-Interchange Kinetics. We have already discussed the temperature dependence of the NMR spectra below about 335 K, but above 335 K in the ^{13}C NMR spectrum and above about 347 K in the ^{31}P NMR spectrum, the resonances broaden with increasing severity as the temperature

(28) The triplet-like form of the spectrum might perhaps have reflected coupling to two different phosphorus atoms for each methyl carbon in a prismatic phosphine ligand, with the coupling constants being of similar magnitude (the best fit of simulated spectra to the experimental data involves coupling constants of 14 and 11 Hz). In this case, the second coupling would have to correspond to a vicinal three-bond $^3J_{CP}$ coupling. Determination of the dihedral angles for the possible three-bond couplings of a methyl carbon of a prismatic phosphine to either the capping phosphorus atom or the other prismatic phosphorus atom in a molecule is complicated by the "tripod" reorientation of the phosphine ligands, but an empirically derived Karplus relationship for some 2-norbornylphosphine compounds suggests that $^3J_{CP}$ will be at a minimum for angles around ≈105°, as prevails here.[29] An alternative mechanism for this invoked coupling could be proposed, namely that the two prismatic phosphines are not magnetically equivalent and may be strongly mutually scalar-coupled. That this coupling is not observed in the ^{31}P CP/MAS NMR spectrum could be rationalized as a consequence of the degeneracy of chemical shifts, and the three-bond vicinal coupling to the nonbonded prismatic phosphorus is, on the basis of this suggestion, then as a result of virtual coupling. However, the observed temperature dependence of the form of the experimental spectra is not simply explained with either of the above models.

(29) Quin, L. D.; Gallagher, M. J.; Cunkle, G. T.; Chestnut, D. B. *J. Am. Chem. Soc.* **1980**, *102*, 3136–3143.

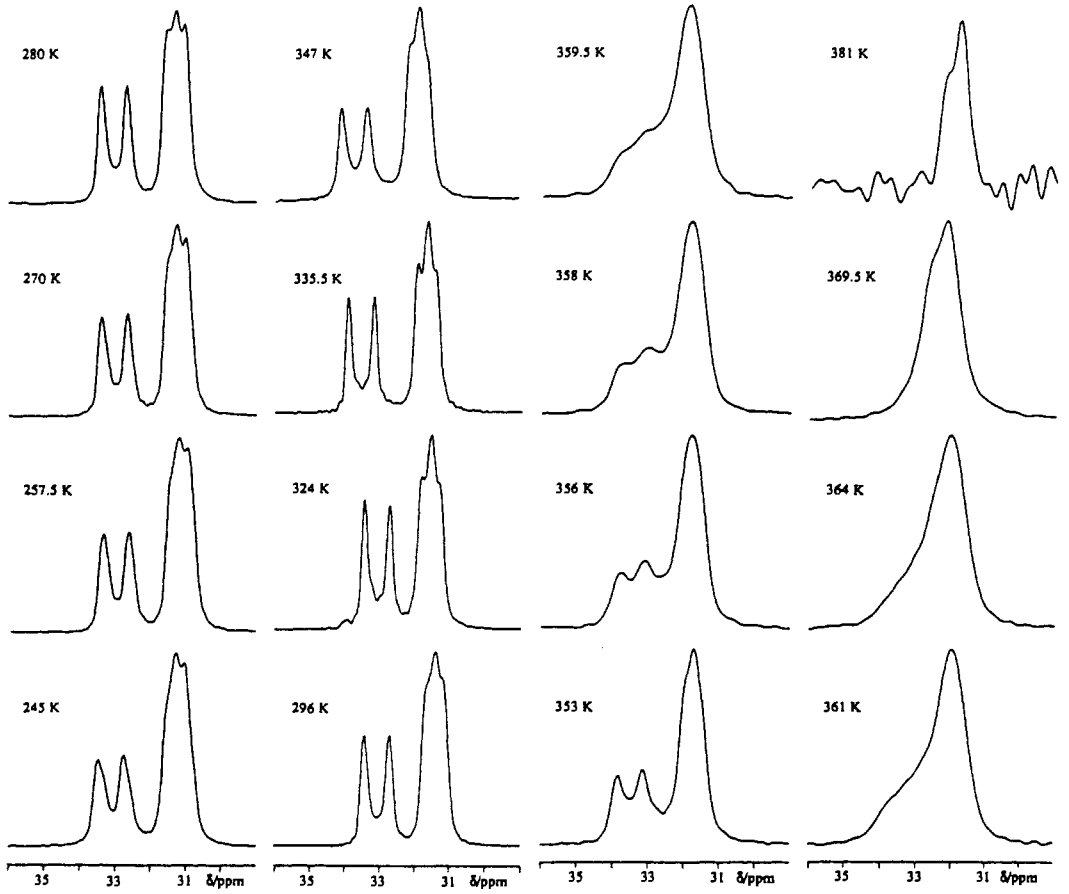

Figure 5. ^{13}C CP/MAS NMR spectra for $W(PMe_3)_3H_6$ in the temperature range 245–381 K.

is elevated (see Figures 5 and 6). At about 361 K, the resonances due to the two methyl regions of the ^{13}C NMR spectrum coalesce to a single averaged resonance that sharpens with further increase in temperature. The ^{31}P NMR resonances broaden increasingly as the temperature rises but do not coalesce before 381 K, above which temperature **1** undergoes thermal decomposition. This behavior indicates that at these higher temperatures chemical exchange between the phosphine environments of **1** reaches a rate in the intermediate region of the exchange-broadening regime. Coalescence at a lower temperature in the ^{13}C NMR spectrum than in the ^{31}P NMR spectrum is a consequence of the smaller frequency separation of the resonances in the former case. The exchange-broadened line shapes for both ^{13}C and ^{31}P NMR spectra were simulated by using the program DNMR4[24] on the basis of a three-site system with coupling constants and relaxation parameters derived from the highest temperature static system amenable to such an analysis for each nucleus.[30] The simulated line shapes are very similar in form to the experimental spectra, and the rate constants for ligand site interchange derived at each temperature from ^{13}C and ^{31}P NMR data agree well (see Figures 5–8). At 381 K, above which temperature **1** undergoes thermal decomposition, the ligand site interchange has just reached rates at which spectral broadening on the MAS scale becomes significant,[31] but no kinetic analysis could be performed in this regime.

The ligand site interchange was probed at lower rates, in the slow limit of the exchange-broadening regime, by one-dimensional magnetization-transfer experiments[19,20] for both ^{13}C and ^{31}P NMR spectra. The rate of magnetization transfer from the more intense resonance at lower chemical shift to the resonance at higher chemical shift was measured in each case. Because no distinction can be made between the two prismatic phosphine environments in such experiments, the data were analyzed on a two-site model with site populations of 2:1 in the prismatic and capping environments, respectively. Following the kinetic treatment for spin exchange of Jeener et al.,[22] it may be shown that if the ratio of the intensity of the originally suppressed resonance at greater chemical shift relative to the selected resonance to lower chemical shift at a mixing time of τ is r, then $\ln [(1 + r)/(1 - 2r)] = k\tau$. A plot of $\ln [(1 + r)/(1 - 2r)]$ against τ should yield a straight line of gradient k, where k is the modified rate constant for ligand site interchange. For ^{13}C NMR spectra, linear plots permitted measurements of k at 324, 335, and 347 K. At 296 K, no magnetization transfer was observed before the short T_1 time of the methyl carbons rendered the ^{13}C NMR resonances unobservable. In the case of the ^{31}P NMR spectra, magnetization transfer rates were obtained in a similar manner at temperatures from 269 to 358 K. At 269 and 296 K, identical rates of exchange of $k = 3.7\ s^{-1}$ were obtained, indicating a temperature-independent contribution to the transfer due to spin diffusion processes, in addition to the temperature-dependent contribution from chemical exchange. The rate of transfer due to spin diffusion was assumed to be temperature-independent, and equal to $3.7\ s^{-1}$, and this value was subtracted from the overall magnetization-transfer rate at each temperature to obtain the contribution arising from chemical exchange alone.

(c) Discussion. The rate data from the simple analysis of exchange broadening and magnetization transfer regimes for both ^{13}C and ^{31}P NMR spectra are presented as a $\ln k$ vs $1/T$ plot in Figure 9 and are also detailed in Table II. Except for the rate values at the low- and high-temperature extremes, which are expected to be the most inaccurate, the data fit well to an Arrhenius relation with the large activation energy of $E_a = 148.8$

(30) The use of the same static site frequencies for simulation at each temperature was forced by the inability to fit the observed temperature-dependent changes in chemical shift at temperatures below the exchange-broadening regime to any simple function. This prevented extrapolation of the chemical shift values for each resonance through the temperature range of spectral simulation. Simulations of spectra produced with differing chemical shift values at each individual temperature suggest that errors in the rates derived at each temperature due to this simplification lie well within the error limits quoted in Table II.

(31) Suwelack, D.; Rothwell, W. P.; Waugh, J. S. *J. Chem. Phys.* **1980**, *73*, 2559–2569.

Table II. Rate Constants for Phosphine Ligand Interchange in $W(PMe_3)_3H_6$

temperature/K	^{13}C magnetization transfer/s^{-1}	^{31}P magnetization transfer/s^{-1} [a]	^{13}C exchange broadening/s^{-1}	^{31}P exchange broadening/s^{-1}
269		... (3.7 ± 0.3)		
296		... (3.7 ± 0.3)		
324	0.8 ± 0.4	2.2 ± 0.9 (5.9 ± 0.6)		
335.5	4.3 ± 0.7	3.0 ± 0.9 (6.7 ± 0.6)	2.0 ± 3.0	2.0 ± 4.0
347	28.5 ± 3.0	20.7 ± 3.0 (24.4 ± 2.7)	22.5 ± 5.0	27.0 ± 3.0
353			55.5 ± 5.0	
356			90.0 ± 8.0	
358		150.8 ± 5.0 (154.5 ± 5.0)	120.0 ● 10.0	180.0 ± 15
359.5			150.0 ± 15.0	
361			195.0 ● 20.0	
364			285.0 ± 20.0	
369.5			650.0 ± 50.0	350.0 ± 40
381			1350.0 ± 200.0	2700.0 ± 300

[a] These figures show the rate of magnetization transfer due to chemical exchange alone (the figures in parentheses are for overall magnetization transfer)—see text.

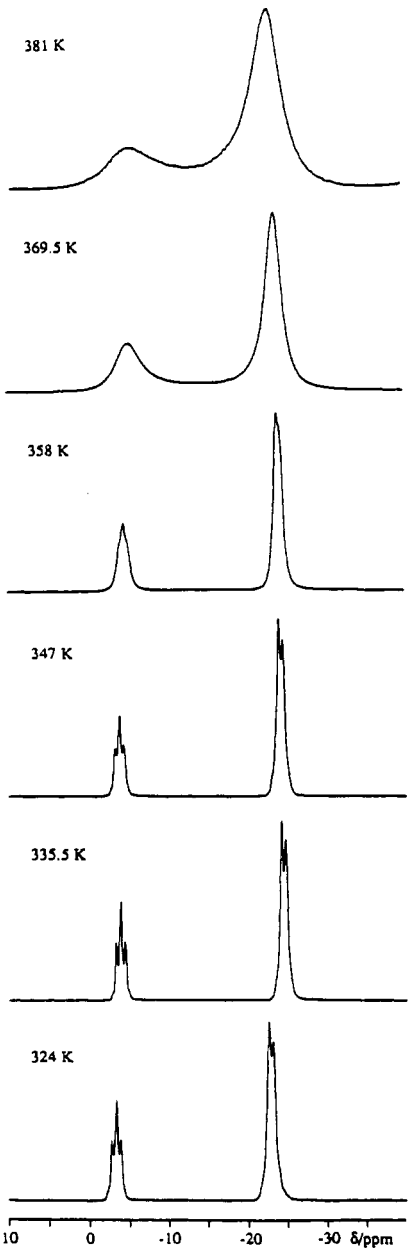

Figure 6. ^{31}P CP/MAS NMR spectra of $W(PMe_3)_3H_6$ in the temperature range 324–381 K.

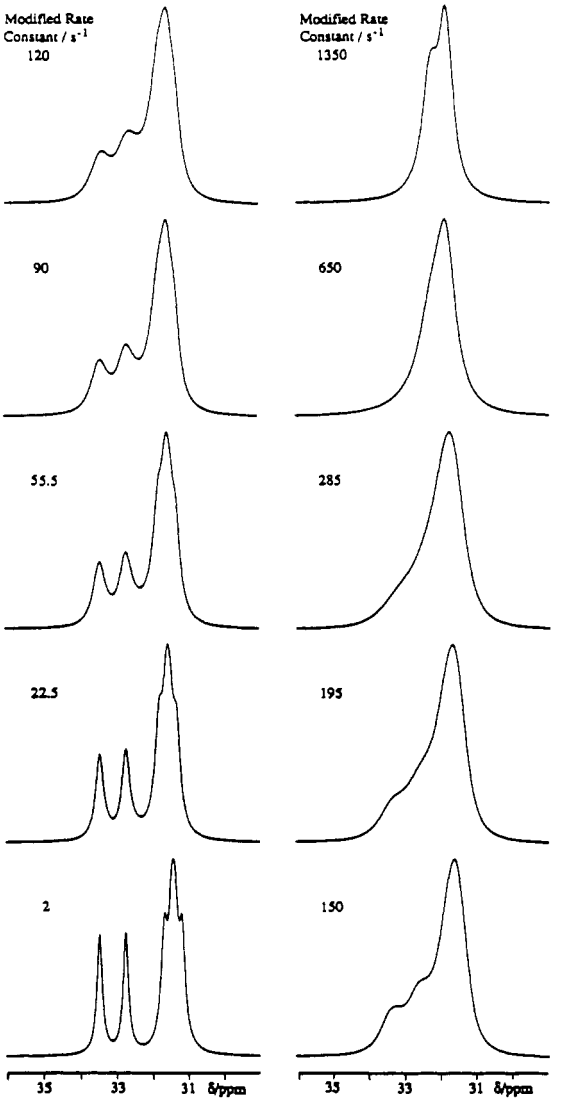

Figure 7. Simulations of the ^{13}C CP/MAS NMR spectra of $W(PMe_3)_3H_6$ using the program DNMR4. A three spin site model was used with one carbon spin and two phosphorus spins, and exchange of the system is restricted to that between two configurations with equilibrium populations in the ratio 2:1, representing the methyl carbon in the prismatic and capping environments, respectively.

± 15 kJ mol^{-1} and an unusually high frequency factor of $A = 6.6 \times 10^{23}$ s^{-1}. The significance of such a large preexponential factor is not understood, but clearly, ligand site interchange is far less facile in the solid state than in solution. This is understandable given the participation of intermolecular packing forces in any barrier to ligand dynamics in solids.

Any mechanism for rearrangement that invokes spatial permutation of the phosphine ligands is very likely to have a high activation barrier in the solid state, in which the major inter-

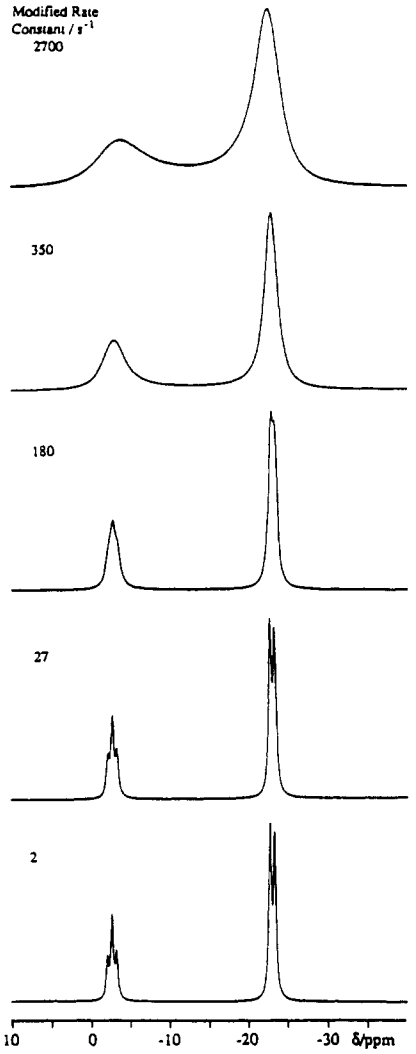

Figure 8. Simulations of the center band of the ^{31}P CP/MAS NMR spectra of $W(PMe_3)_3H_6$ using the program DNMR4. A three-site model corresponding to the three ^{31}P spins was used, allowing mutual exchange between sites.

molecular interactions are expected to be between the relatively bulky phosphine ligands. Many such processes, however, might be expected to have barriers substantially greater than that observed in the experiment reported here. Ligand site interchange may, however, be effected without major alteration of the topological relationship of individual ligands by the TTP ⇌ MSA ⇌ TTP rearrangement generally invoked to explain the fluxionality observed in solution (see Figure 1). Analysis of such a rearrangement for the structure implicated here reveals that if the polyhedral edge stretch performed to reach the MSA intermediate is of the edge connecting the eclipsed prismatic phosphines, on relaxation of the MSA transition state the alternative TTP geometry involves the three phosphines occupying capping positions. The alternative prismatic edge stretches involving hydride ligands lead, on relaxation of the transition state, to alternative TTP geometries where the three phosphines occupy inequivalent prismatic sites. Both such geometries are likely to be of higher energy than the ground-state geometry, and so their equilibrium populations must be lower. If we consider the former case, the new TTP structure may be returned to the original topology by any of the three similar polyhedral edge stretches, each involving one prismatic hydride and one prismatic phosphine ligand. One of these stretches simply duplicates the original disposition of the phosphine ligands; the other two lead to identical coordination topology, but with a different molecular orientation to the crystalline frame, such that there is a functional interchange of labeled ligands (i.e., pseudorotation of the molecule has occurred). Such a "double-stretch" rearrangement is illustrated in Figure 10. Thus

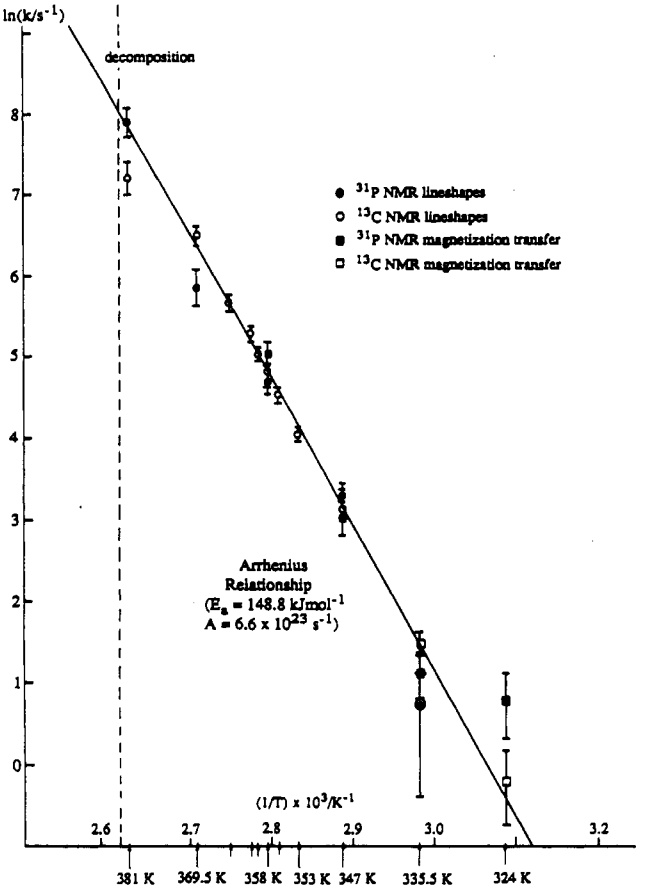

Figure 9. Arrhenius plot for ligand functionality interchange in $W(PMe_3)_3H_6$ showing the rate data from NMR magnetization transfer and exchange broadening experiments.

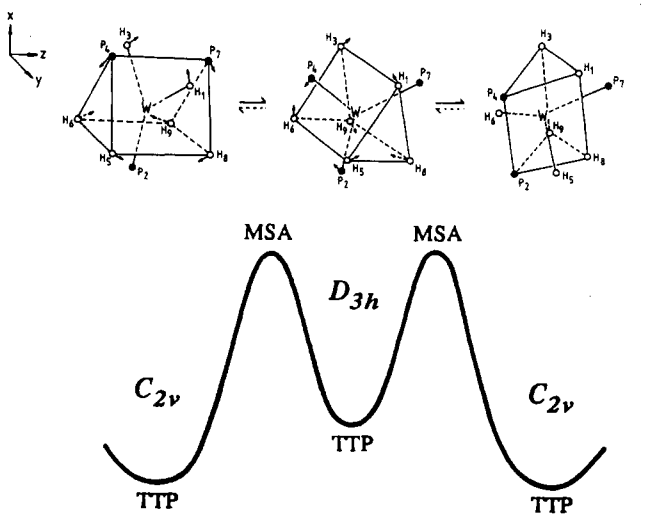

Figure 10. Energy profile for the rearrangement and the proposed "double-stretch" mechanism that effects ligand functionality interchange.

successive transitions through the TTP geometry in which all phosphine ligands are in capping positions (incidentally the geometry originally predicted for these compounds and probably not excessively higher in energy than the ground state configuration) allows complete scrambling of the ligand functionality. Furthermore the spatial movement of the phosphine ligands relative to the crystalline frame need only be relatively small and so involves minimum disruption to the intermolecular interactions in the solid state. As the temperature is increased, other pathways might become populated too, perhaps involving other prismatic edge stretches that create TTP topologies with different ar-

rangements of phosphine ligands and require passage through several intermediate TTP topologies in order to return to the ground-state arrangement with two eclipsed prismatic phosphines and a capping phosphine on the opposite prismatic face.

Conclusions

^{13}C and ^{31}P CP/MAS NMR data obtained over a range of temperatures are consistent with a tricapped-trigonal-prismatic structure for $W(PMe_3)_3H_6$, with two phosphine ligands in eclipsed prismatic sites and the third in the opposite capping site. In contrast to the results of previous crystallographic studies on such compounds, the NMR spectra suggest that the two prismatic phosphine ligands in each molecule are slightly inequivalent. At temperatures above ambient, interchange of ligand functionality for the phosphine ligands is observed by magnetization-transfer experiments and, at still higher temperatures, by simulation of the exchange-broadened NMR line shapes observed experimentally. Rate data from the two methods of analysis suggest Arrhenius activation parameters for ligand functionality interchange of $E_a = 148.8 \pm 15$ kJ mol^{-1} and $A = 6.6 \times 10^{23}$ s^{-1}. The rate of functionality interchange reaches ca. 2000 Hz by the decomposition point of the material (381 K). A mechanism for this exchange has been proposed, involving the "double rearrangement"

$$\text{TTP(ground state)} \rightleftharpoons \text{MSA} \rightleftharpoons \text{TTP(excited state)} \rightleftharpoons \text{MSA} \rightleftharpoons \text{TTP(ground state)}$$

In this mechanism slight stretches of the polytypal edges result in interchange of ligand functionality without the need for unfavorable spatial permutation of the phosphine ligands.

Acknowledgment. J. Pound is thanked for a sample of $W(PMe_3)_3H_6$, and Drs. J. M. Twyman, D. O'Hare, L. L. Wong, and A. Sella are thanked for valuable assistance and advice. The SERC is thanked for financial support.

Contribution from the Departments of Chemistry, University of Minnesota, Minneapolis, Minnesota 55455, and University of New Orleans, New Orleans, Louisiana 70122

Models for Diiron–Oxo Proteins: The Peroxide Adduct of $Fe_2(HPTB)(OH)(NO_3)_4$

Bridget A. Brennan,† Qiuhao Chen,† Carlos Juarez-Garcia,† Anne E. True,† Charles J. O'Connor,‡ and Lawrence Que, Jr.*,†

Received October 23, 1990

The complex of $Fe(NO_3)_3$ and *N,N,N',N'*-tetrakis(2-benzimidazolylmethyl)-2-hydroxy-1,3-diaminopropane (HPTB) is reformulated as $[Fe_2(HPTB)(\mu\text{-}OH)(NO_3)_2](NO_3)_2$ on the basis of ^1H NMR, EXAFS, X-ray diffraction, and conductivity data. This complex reacts with hydrogen peroxide to form a 1:1 adduct with a new charge-transfer band at 600 nm ($\epsilon = 1500$ M^{-1} cm^{-1}). Resonance Raman studies show two resonance-enhanced vibrations, $\nu_{Fe\text{-}O}$ at 476 cm^{-1} and $\nu_{O\text{-}O}$, which appears as a Fermi doublet centered at 895 cm^{-1}; these features shift to 457 and 854 cm^{-1}, respectively, with the use of $H_2{}^{18}O_2$ but are not affected by D_2O. ^1H NMR measurements indicate that the antiferromagnetic coupling is increased from $-J = 20$ cm^{-1} to ca. 70 cm^{-1} upon formation of the peroxide adduct, suggesting the introduction of a new coupling pathway. The ^{57}Fe Mössbauer spectrum of the peroxide complex reveals a quadrupole doublet ($\delta = 0.54$ mm/s, $\Delta E_Q = 0.84$ mm/s) distinct from that of the precursor complex ($\delta = 0.49$ mm/s, $\Delta E_Q = 0.66$ mm/s), indicating that the two irons are affected similarly by peroxide binding. Conductivity measurements in CH_3CN show that the adduct is a 1:1 electrolyte. Taken together, the physical data suggest the formulation $[Fe_2(HPTB)(\mu\text{-}\eta^1\text{:}\eta^1\text{-}O_2)(NO_3)_2](NO_3)$ for the peroxide complex. Such dinuclear iron peroxide complexes may be relevant to putative intermediates in the oxygenation of the reduced forms of ribonucleotide reductase and methane monooxygenase.

Diiron centers that are known to interact with dioxygen[1] have been found in hemerythrin,[2] methane monooxygenase,[3,4] and ribonucleotide reductase.[5-7] Deoxyhemerythrin reversibly binds dioxygen and has an active site consisting of a (μ-hydroxo)bis(μ-carboxylato)diiron(II) core and five terminal histidines. Dioxygen binds to the diferrous center at the remaining vacant coordination site with concomitant electron and proton transfer, forming a (μ-oxo)diferric center with a coordinated hydroperoxide moiety that is hydrogen-bonded to the oxo bridge (Figure 1).[8,9] Dioxygen may bind in similar or related fashion to the diferrous centers of methane monooxygenase and ribonucleotide reductase to effect the necessary oxidative chemistry associated with these enzymes.[4,10]

Because a number of ligand systems[11-16] have been used successfully to model the spectroscopic and structural properties of the diferric sites in the crystallographically characterized azidomethemerythrin[17] and ribonucleotide reductase,[18] emphasis is now shifting toward efforts that model the diferrous–dioxygen/diferric–peroxide chemistry exhibited by these proteins. While there are a number of examples of structurally characterized dinuclear cobalt and copper peroxide complexes,[19-23] no nonheme diferric peroxide complex is comparably well characterized. Dioxygen adducts of three ferrous complexes are known; that of $[Fe(pyN5)]^{2+}$[24] has only been cursorily characterized,[25] while the adducts of $[Fe\{HB(3,5\text{-}i\text{-}Pr_2pz)_3\}(OBz)]$[26] and $[Fe_2(N\text{-}Et\text{-}HPTB)OBz]^{2+}$[27] are proposed to have (μ-η^1,η^1-peroxo)diiron(III) units on the basis of spectroscopic data. (μ-Peroxo)diiron(III)

†University of Minnesota.
‡University of New Orleans.

(1) Que, L., Jr.; True, A. E. *Prog. Inorg. Chem.* **1990**, *38*, 97–200.
(2) Klotz, I. M.; Kurtz, D. M., Jr. *Acc. Chem. Res.* **1984**, *17*, 16–22. Sanders-Loehr, J.; Loehr, T. M. *Adv. Inorg. Biochem.* **1979**, *1*, 235–252.
(3) Woodland, M. P.; Patil, D. S.; Cammack, R.; Dalton, H. *Biochim. Biophys. Acta* **1986**, *873*, 237–242.
(4) Fox, B. G.; Froland, W. A.; Dege, J. E.; Lipscomb, J. D. *J. Biol. Chem.* **1989**, *264*, 10023–10033. Fox, B. G.; Surerus, K. K.; Münck, E.; Lipscomb, J. D. *J. Biol. Chem.* **1988**, *263*, 10553–10556.
(5) Reichard, P.; Ehrenberg, A. *Science (Washington, D.C.)* **1983**, *221*, 514–519.
(6) Lynch, J. B.; Juarez-Garcia, C.; Münck, E.; Que, L., Jr. *J. Biol. Chem.* **1989**, *264*, 8091–8096.
(7) Sahlin, M.; Gräslund, A.; Petersson, L.; Ehrenberg, A.; Sjöberg, B.-M. *Biochemistry* **1989**, *28*, 2618–2625.
(8) Shiemke, A. K.; Loehr, T. M.; Sanders-Loehr, J. *J. Am. Chem. Soc.* **1984**, *106*, 4951–4956.
(9) Stenkamp, R. E.; Sieker, L. C.; Jensen, L. H.; McCallum, J. D.; Sanders-Loehr, J. *Proc. Natl. Acad. Sci. U.S.A.* **1985**, 713–716.
(10) (a) Fontecave, M.; Eliason, R.; Reichard, P. *J. Biol. Chem.* **1989**, *264*, 9164–9170. (b) Fontecave, M.; Gerez, C.; Atta, M.; Jeunet, A. *Biochem. Biophys. Res. Commun.* **1990**, *168*, 659–664. (c) Sahlin, M.; Sjöberg, B.-M.; Backes, G.; Loehr, T.; Sanders-Loehr, J. *Biochem. Biophys. Res. Commun.* **1990**, *167*, 813–818.
(11) Armstrong, W. H.; Spool, A.; Papaefthymiou, G. C.; Frankel, R. B.; Lippard, S. J. *J. Am. Chem. Soc.* **1984**, *106*, 3653–3667.
(12) Wieghardt, K.; Pohl, K.; Gebert, K. *Angew. Chem., Int. Ed. Engl.* **1983**, *22*, 727–728.
(13) Toftlund, H.; Murray, K. S.; Zwack, P. R.; Taylor, L. F.; Anderson, O. P. *J. Chem. Soc., Chem. Commun.* **1986**, 191–192.
(14) Gomez-Romero, P.; Casan-Pastor, N.; Ben-Hussein, A.; Jameson, G. B. *J. Am. Chem. Soc.* **1988**, *110*, 1988–1990.

0020-1669/91/1330-1937$02.50/0